Investigation on Inlet Recirculation Characteristics of Double Suction Centrifugal Compressor with Unsymmetrical Inlet

YANG Ce[1,*], WANG Yingjun[1], LAO Dazhong[2], TONG Ding[3], WEI Longyu[1], LIU Yixiong[1]

1. School of Mechanical Engineering, Beijing Institute of Technology, Beijing, 100081, China
2. School of Aerospace Engineering, Beijing Institute of Technology, Beijing, 100081, China
3. China North Engine Research Institute, Tianjin, 300405, China

The inlet recirculation characteristics of double suction centrifugal compressor with unsymmetrical inlet structures were studied in numerical method, mainly focused on three issues including the amounts and differences of the inlet recirculation in different working conditions, the circumferential non-uniform distributions of the inlet recirculation, the recirculation velocity distributions of the upstream slot of the rear impeller. The results show that there are some differences between the recirculation of the front impeller and that of the rear impeller in whole working conditions. In design speed, the recirculation flow rate of the rear impeller is larger than that of the front impeller in the large flow range, but in the small flow range, the recirculation flow rate of the rear impeller is smaller than that of the front impeller. In different working conditions, the recirculation velocity distributions of the front and rear impeller are non-uniform along the circumferential direction and their non-uniform extents are quite different. The circumferential non-uniform extent of the recirculation velocity varies with the working conditions change. The circumferential non-uniform extent of the recirculation velocity of front impeller and its distribution are determined by the static pressure distribution of the front impeller, but that of the rear impeller is decided by the coupling effects of the inlet flow distortion of the rear impeller, the circumferential unsymmetrical distribution of the upstream slot and the asymmetric structure of the volute. In the design flow and small flow conditions, the recirculation velocities at different circumferential positions of the mean line of the upstream slot cross-section of the rear impeller are quite different, and the recirculation velocities distribution forms at both sides of the mean line are different. The recirculation velocity distributions in the cross-section of the upstream slot depend on the static pressure distributions in the intake duct.

Keywords: asymmetric intake, double suction centrifugal compressor, inlet recirculation, recirculation flow, circumferential distribution

Introduction

Compared with the conventional compressor, the double suction centrifugal compressor has the advantages of wide flow range and relatively small size [1]. The turbocharger equipped with the double suction centrifugal compressor, can improve the matching relation between the compressor and the turbine, thereby allowing the tur-

Nomenclature

η	compressor efficiency	$\bar{V}$	average velocity
π	pressure ratio	*Norm.*	normalized
m	mass flow	*Recir.*	recirculation
max	maximum	RANS	Reynolds-Averaged Navier-Stokes
min	minimum	S-A	Spalart-Allmaras

L	left side	IGG	interactive grid generator
R	right side	**Subscripts**	
p	static pressure	θ	circumferential angle
$\overline{P}$	average static pressure	r	radial direction
V	velocity	z	axial direction

bine working in closer proximity to the optimum speed ratio, which is an effective method for further improving the performance of the turbocharger. Study results show that the turbocharger equipped with a double suction centrifugal compressor can be matched with the engine in a better working condition, showing the advantages of the double suction centrifugal compressor in the application of the turbocharger [2].

The double suction centrifugal compressor usually adopts the back to back structure, a common back plate is set on both sides of the impeller. In application of the double suction centrifugal compressor in the turbocharger, the impeller away from the intermediate side uses a straight inlet duct to ensure the axial intake, and this side of the impeller is called the front impeller. The other side of the impeller near the intermediate, leading to the intake of this side of the impeller along the radial direction and the impeller inlet is connected with complex shaped bent duct, called the rear impeller. Because the rear impeller is connected with the bent inlet duct, the flow loss in the bent duct is inevitable, and the distortion flow field is formed at the impeller inlet. The different inlet flow fields on both sides of the impeller makes the work pattern of the double suction centrifugal compressor has some special characteristics. Studies have found that the flow rate of front impeller is always larger than that of the rear impeller in the stable working range. With the total flow rate decreases, the flow rate difference between the front and rear impeller increases. When the total flow rate of the compressor reaches to a certain extent, a wide separation range appears in the rear impeller passage, and the flow rate of the rear impeller is very small, the flow ratio of the front and rear impeller is larger than 2, at this moment, the rear impeller does not apply work on the airflow, and the rear impeller is in an inert state. The working mode of the double suction compressor converts from the two sides of the impeller parallel working state into the front impeller working alone [3, 4].

The recirculation device is an effective method to broaden the stable working range of the centrifugal compressor, which is widely used in the centrifugal compressor. A recirculation device is generally arranged on the casing wall, which consists of an upstream slot, a bleed slot and an annular cavity connecting both slots. Wherein, the recirculation slot arranged on the upstream of the impeller is called upstream slot, the other recirculation slot set on the downstream of the leading edge of the blade is called bleed slot. In the large flow condition, the pressure in the bleed slot is lower than external pressure, the air flows through the recirculation slot and the refluxing cavity then flows into the blade passage. The flow rate increase of compressor depends upon the recirculation flow from bleed slot, and this achieves the purpose of increasing the flow area of impeller inlet [5]. In the small flow condition, the pressure in bleed slot is higher than external pressure, the airflow flows away the blade passage from bleed slot, then outflows through the refluxing cavity and upstream slot, thus produces a recirculation region in the impeller inlet. This increases the actual flow rate of blade leading edge, makes the incidence angle of the blade leading edge at the inlet tip region decreases and reduces the airflow fluctuation amplitude significantly near stall condition [6, 7].

Researches about the recirculation device have been carried out. Such as Harley et al. [8] improved the meanstreamline model of the inlet recirculation, considering the direct effects of the recirculation, which simulated the performance of centrifugal compressor with inlet recirculation more accurately. Tamaki [9] studied the effects of upstream slot and bleed slot on the flow field of the blade passage. The results showed that the bleed slot reduces the blade loading at the impeller tip region. The tip leakage flow exiting the bleed slot becomes lower than that without the recirculation device. Moreover, the bleed slot changes the position of the shock near downstream of the bleed slot. Chen [10] and Tamaki [11] studied the performance change of centrifugal compressor in the case that the recirculation cavity is arranged with guide vanes. Installing guide vanes in the recirculation cavity can remove the pre-swirl from the port flow to minimize mixing loss with the main flow. A reasonable design of the guide vane can further reduce the mass flow rate of surge. Tamaki et al [12] studied the effects of inlet recirculation on the performance of turbocharger centrifugal compressor by one-dimensional flow method, proposing a method of using small fins mounted in a compressor-inlet duct to control the flow at recirculation zone of blade leading edge near the blade tip in small flow conditions. The experimental results indicate that this method can be used to further reduce the surge flow rate in low compressor-speed conditions. Hunziker et al [13] conducted an optimization design for the geometry structure of inlet recirculation. Hu [14] et al designed a double bleed slot. Different recirculation slot is closed with the working

condition changes, which effectively solves the efficiency drop of centrifugal compressor caused by the inlet recirculation. Gancedo [15] measured the flow field of centrifugal compressor near inlet recirculation using PIV approach. The experimental results showed that the flow field structure is similar in the case that there is a recirculation or without the recirculation device in the large flow and the design flow conditions, but in the near stall condition, the flow field structures are different. Such studies of centrifugal compressor inlet recirculation device mainly focus on the mechanism of inlet recirculation to broaden the operating range, on the flow field of compressor with recirculation device, on the geometry determination of recirculation device, and the mathematical calculation model of centrifugal compressor performance considering the recirculation device.

The flow field is asymmetric along the circumferential direction inside the centrifugal compressor. There is a difference in the flow rate of each blade passage, which means that every blade passage works in different operating conditions. Moreover, the asymmetric flow field also makes the different distribution of the circumferential recirculation flow. Tamaki et al. [16] proposed the bleed slot with non-axisymmetric arrangement in the circumferential direction. Experimental results showed that the characteristic of compressor varies with changes in the circumferential non-axisymmetric distribution of the bleed slot. The stall flow rates of the compressor with circumferential non-axisymmetric bleed slot have a decreasing trend. The asymmetric flow field in the centrifugal compressor is caused by the structure of the volute. Studies on conventional and double suction centrifugal compressor have found that the static pressure distribution in the volute is asymmetric in circumferential direction. The static pressure in the volute increases from the volute tongue to outlet along the streamline direction in small flow condition, and the volute plays the similar role of diffuser. But the static pressure distribution is inversed in large flow condition and the volute plays a similar role of nozzle [17-20]. In large flow conditions, the circumferential static pressure gradient is the maximum, and the static pressure gradient decreased with the flow rate. The circumferential static pressure distribution in the diffuser has the same distribution form as the volute. For a certain flow condition, the non-uniform extent of the static pressure distributions in the diffuser at different radii are basically the same [20].

For the rear impeller of the double suction centrifugal compressor, the internal non-axisymmetric flow field is affected by the inlet distortion besides the influence of the shape of the volute. Therefore, compared with the conventional centrifugal compressor, the non-axisymmetric flow field in the rear impeller is formed under the coupling effects of the inlet distortion flow field and the non-axisymmetric structure of the volute [20]. Moreover, the flow distortion caused by the rear impeller inlet bent duct will also increases the flow losses in the diffuser. The flow loss in a double suction centrifugal impeller was studied in reference [21]. It found that the additional flow loss will be produced in the diffuser due to the total pressure difference between the front and rear impeller inlet, and the flow loss increases with the total pressure difference enhances. In large flow conditions, the main flow loss in the diffuser came from the flow mixing of both sides of the impeller. In small flow conditions, the separation vortex at diffuser wall surface is intensified, the separation vortex loss is significantly larger than the flow mixing loss on both sides of the impeller, and the diffuser loss increases with the inlet difference of both sides of the impeller strengthens. Due to the work capacity of rear impeller in small flow condition is less than that of front impeller, resulting in the working mode of double suction centrifugal compressor converting from both sides of impeller work together to the front impeller work alone. Jing [22] proposed a method of supplying the acting ability of rear impeller by increasing the radius of rear impeller to suppress the rear impeller to enter into stall condition untimely, so as to widen the double suction compressor operating range. The results showed that there is an optimum radius of the rear impeller to match the front and rear impeller working in a stable range. And the stability operating range of the double suction impeller is narrow with both insufficient and excessive increasing the radius of the rear impeller. In summary, studies on the double suction centrifugal compressor mainly focused on the working mode conversion process and mechanism, the flow rate distribution of front and rear impeller in different working conditions, the circumferential non-uniform flow field distribution phenomenon and formation. Few attention was paid to the inlet recirculation of the double suction centrifugal compressor with asymmetric inlets.

There are significant differences in the internal flow field structures between the asymmetric inlets double suction centrifugal compressor and conventional centrifugal compressor. Especially for the rear impeller of double suction compressor, some special flow phenomena are produced due to the circumferential distribution characteristics of the flow field in the rear impeller affected by the non-symmetric volute and bent inlet duct. Meanwhile, the recirculation device of the rear impeller is in significant difference with that of the conventional compressor. In the coupled effects of these factors, the recirculation flow of the rear impeller will be different from that of the single-sided impeller. This paper mainly focuses on the recirculation flow rate distribution characteristics of the front and rear impeller and quantitatively describes the difference of the recirculation flow

rate of both side impeller in different working conditions. In typical operating condition, the circumferential distribution form of the flow rate of two sides of impeller was given and the forming mechanism was analyzed. The recirculation flow rate difference of the upstream slot of rear impeller at the two inlet branch ducts was compared. And the circumferential flow rate distribution characteristics of the recirculation flow of rear impeller at the two inlet branch ducts of the upstream slot position were obtained by analyzing the circumferential distribution form of the flow parameters of the upstream slot of rear impeller on the inlet cross section.

Model description

A double suction centrifugal compressor was adopted in this paper, and the main region of the impeller as shown in Fig. 1, including the inlet ducts, double suction impeller, both sides of impeller inlet recirculation device, sharing vaneless diffuser, volute and outlet ducts. Because the turbocharger is limited to the limited installation form and space size of the engine structure arrangement, the inlets on both sides of impellers are supplied from a common inlet duct. There is a significant difference in the inlet forms for the double suction impeller, where the front impeller is the axial intake, and the intake of the rear impeller is achieved by the bent bending duct. The airflow is divided into two parts after entering the import duct: the part airflow one is along the straight duct enters into the front impeller, and the other airflow to the rear impeller along the branch duct which is then divided into the left and right inlet ducts and finally enters into the rear impeller passage. The gases are pressurized by both sides of the impeller and then flow into the sharing diffuser and finally collected by the volute.

The inlet recirculation structures of the double suction centrifugal compressor can be seen from Fig. 1. Obviously, the recirculation device of the front and rear impeller is of significant difference. Fig. 2 shows the enlarged view of the recirculation device region. It can be seen that the inlet recirculation device of the front impeller is the same with that of the traditional centrifugal compressor, the upstream slot locates at impeller upstream, the bleed slot locates at the impeller inlet axial section, and both of them are with annular structures. For the rear impeller, the recirculation device is still connected with annular cavity. But the inlet duct of the rear impeller is divided by two intake branches due to the limited structure of double suction compressor. The upstream slot of the rear impeller is set by a portion of annular cavity, as shown in Fig. 3. Fig. 4 is the schematic diagram of the upstream slot of the rear impeller with respect to the impeller circumferential position, the arc

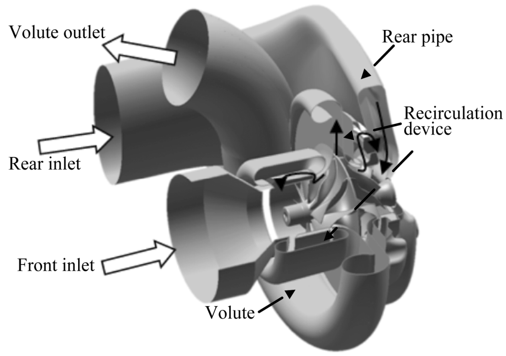

Fig. 1 Sectional view of the main area of the double suction centrifugal compressor impeller

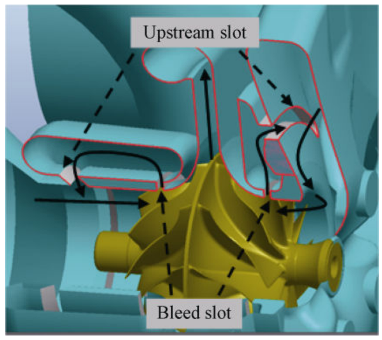

Fig. 2 Recirculation device of front and rear impellers

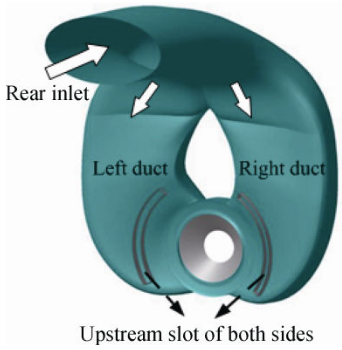

Fig. 3 Upstream slot of the rear impeller

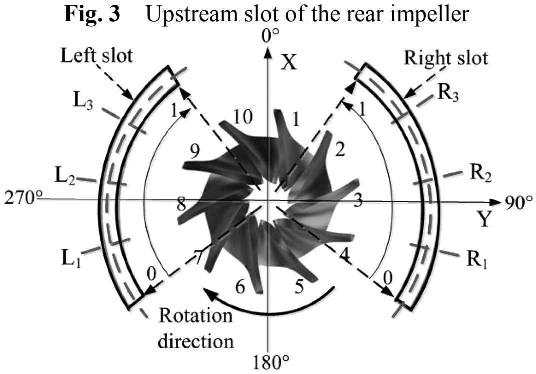

Fig. 4 Scheme view of upstream slot of the rear impeller, mean line of the slot and the cross-section position

position and three selected circumference positions of the upstream slot are marked in the figure.. In following discussion, the recirculation flow velocity distributions at these positions will be analyzed.

Calculation grids

To make the calculation domain match well with the actual flow field of double suction compressor, the selected calculation domain includes front and rear inlet duct, intake bent duct of rear impeller, inlet recirculation device, the impeller, volute and outlet duct. The whole calculation domain of the double suction compressor is complex, which can be divided into rotor part of the impeller and stator part of other components. The grids of the stator parts and the front and rear impeller are generated separately, and then assembled into the whole model using the IGG module. In the process of mesh, the adjacent blocks in the same direction are set with proper node number, and the wall surface y^+ value is less than 10. The grids of stator parts such as volute and inlet pipe are meshed manually using IGG module, and the grids of the impellers with the symmetric structure are automatically generated by Autogrid module.

Because of the huge grid number of the whole double suction centrifugal compressor model, validating the grid independence of overall unit is not easy. Therefore, the whole computational domain of double suction centrifugal compressor is divided into several regions in accordance with the modularization method, the regional grids are validated step by step. Firstly, the grid independence of the double impeller without the inlet and outlet duct is conducted. Then, the impeller grids satisfied the independence requirements are used to match different volute grids to determine grid independence of the volute. The inlet and outlet ducts grids are validated separately, and then connected with the volute and compressor. Finally, the grids of whole calculation model including: the front and rear inlet duct with 0.85 million grids, the front impeller and the inlet recirculation structure with 7.60 million grids, the rear impeller and the inlet recirculation structure with 7 million grids, the volute with 1.55 million grids, and the total grids of the double suction centrifugal compressor model is almost 17 million. The grids are as shown in Fig. 5 and Fig. 6.

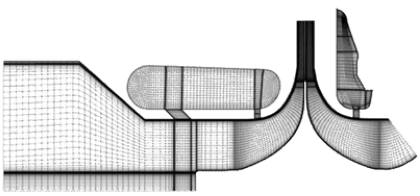

Fig. 5 Meridional grid of double suction impellers

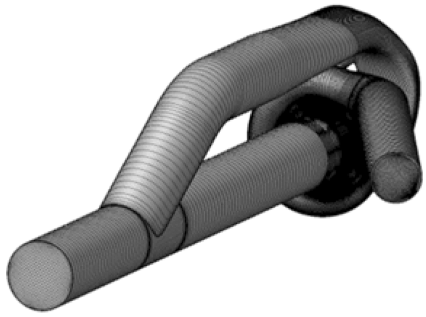

Fig. 6 Grids of double suction centrifugal compressor

Numerical calculation method

The FINE/Turbo software was adopted to solve the steady RANS equations. In the numerical calculation, the S-A turbulence model and the finite volume center discrete method were used. The space discrete used the central scheme; the time term used the explicit four-stage Runge-Kutta scheme for iteration solutions. The multi-grids and residual smoothing methods were adopted to accelerate the convergence of the numerical calculation. Ideal gas was assumed in the computation process, all solid surfaces were treated by the adiabatic and non-slip boundaries. The flow direction of the compressor inlet was along the axial direction. The uniform total pressure and total temperature at the inlet and the static pressure at the outlet were imposed, and the static pressures were increased gradually to simulate the different operating conditions. When the flow reduced to a critical value, the mass flow was given as the outlet condition instead of the static pressure. For the rotor-stator interface, the "frozen-rotor" approach was chosen because the calculation model used the integer cycle impeller passage grids and the inlet recirculation of rear impeller was non-annular structure. Four operating speed conditions were calculated. The design speed of the compressor is 97 kr/min. The relative flow rate is defined as the ratio of the actual flow to the design flow. The performance characteristics of the double suction compressor are obtained as shown in Fig. 7, wherein, Fig. 7 (a) are the efficiency and flow characteristic curves, Fig. 7 (b) are the pressure ratio and flow characteristic curves. In the calculation process, the relative circumferential positions of the rotor and volute are different, and the calculation results at different circumferential positions are compared and analyzed. The results show that the difference of the internal flow structure and performance are very small.

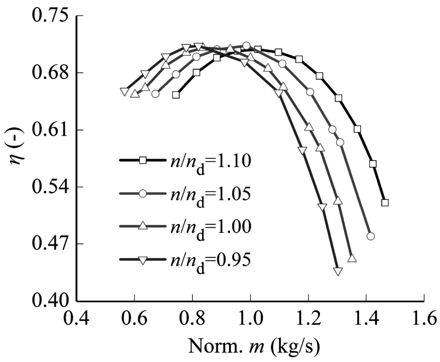

(a) Efficiency and flow

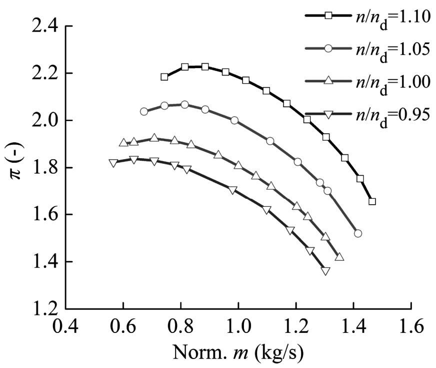

(b) Pressure ratio and flow

Fig. 7 Calculation performance of double suction centrifugal compressor

Results and discussion

Recirculation flow distributions and differences of front and rear impeller

The flow rate through the recirculation channel is defined by the recirculation flow. When the compressor works in the large flow condition, the pressure in the bleed slot is below the pressure at the impeller inlet, so that the air flows into the impeller internal through the bleed slot, and the recirculation flow is negative. In the small flow rate condition, the pressure in bleed slot is higher than the pressure at the impeller inlet, the air flows out from the impeller passage through the bleed slot, and the recirculation flow is positive. Fig. 8 (a) shows the change of the recirculation flow in four different speed conditions, and the recirculation flows at 7 monitor points are showed, respectively, marked with the letters of A, B, C, D, E, F, G. It can be seen from Fig. 8 (a) that the recirculation flow is changed from negative to positive with the back pressure increases and the flow rate of compressor decreases. In B working condition, the recirculation flow reaches the maximum. From condition B to condition A, the recirculation flow rate decreases slightly due to the pressure in bleed slot reduces.

Fig. 8 (b) shows the relative recirculation flow rate, which is defined as the ratio of the recirculation flow rate and the impeller outlet flow rate. It can be seen that the recirculation flow rate of the front impeller can reach 15.9% of its impeller flow rate in the given four speed conditions. At the same speed, the relative recirculation flow rate increases with the flow rate of the compressor decreases from condition E to condition B. From condition B to condition A, the relative recirculation flow rate reduces slightly. Although the total flow of the compressor decreases, but the flow through the front impeller flow increases. Therefore, the relative recirculation flow rate still reduces. In small flow, the pressure difference between the upstream slot and the bleed slot determines the recirculation flow.

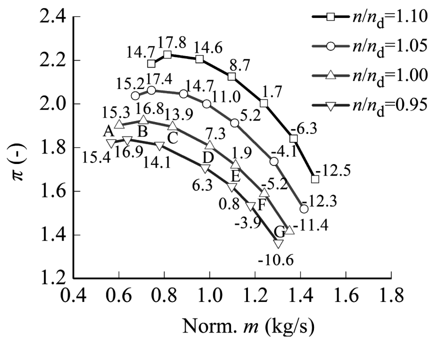

(a) Absolute recirculation flow (10^{-3} kg/s)

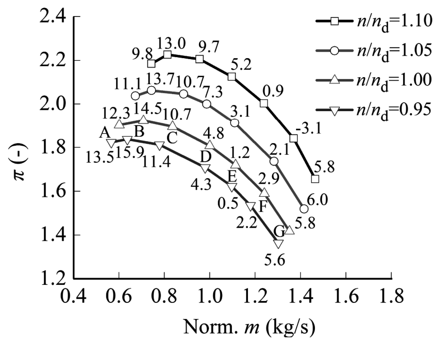

(b) Relative recirculation flow (10^{-3} kg/s)

Fig. 8 Recirculation flow rate of front impeller at different operating conditions

Fig. 9 (a) shows the change of the recirculation flow rate of rear impeller in four different speed lines. The recirculation flow rate of rear impeller changes from negative to positive with the compressor flow decreases. The recirculation flow rate of the rear impeller reaches the maximum at condition A, but the maximum recirculation flow of the front impeller corresponds to condition B and decreases at condition A. Fig. 9 (b) describes that the recirculation flow rate of the rear impeller is about 35.2% of the total flow rate of the rear impeller in the small flow condition, which is much larger than the maximum of the front impeller. This is because the flow rate of the rear impeller decreases and the recirculation

flow rate of the rear impeller increases in the small flow range, the relative recirculation flow rate increases significantly. Additionally, the recirculation flow rate of the rear impeller working at four speeds in A condition has the decreasing tendency.

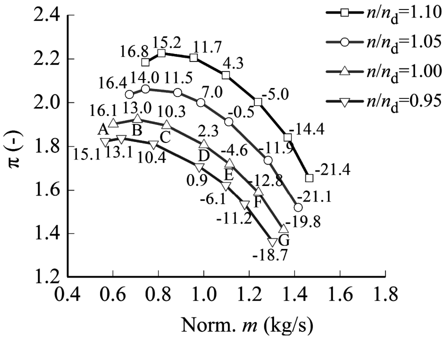

(a) Absolute recirculation flow (10^{-3} kg/s)

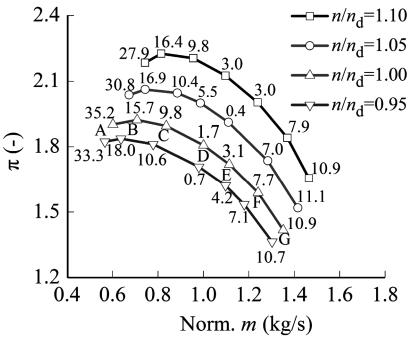

(b) Relative recirculation flow (10^{-3} kg/s)

Fig. 9 Recirculation flow rate of rear impeller at different operating conditions

Fig. 10 shows the absolute recirculation flow rate curves of the front and rear impeller with the total flow change of the compressor in design speed condition. In the figure, the three typical operating conditions are marked, and the H point is the boundary points of the large flow and small flow area, the right side of the H point is large flow range area, the left side of the H point is small flow range area. It can be seen from Fig. 10 that the recirculation flow rates of the front and rear impeller are of significant difference. On the right side of the H point, the negative recirculation flow rate represents that the air flowed into the impeller passages through the recirculation device, and the recirculation flow rate of the rear impeller is larger than that of the front impeller. In the small flow range of the left side of the H point, the positive recirculation flow rate indicates that the air flowed out to the inlet from the impeller passages, and the recirculation flow rate of the front impeller is larger than that of the rear impeller. The results in Fig. 10 show that the recirculation flow rate of front and rear impeller is converted from negative to positive in different flow rate of the compressor, and the converted operating point from negative to positive of the front impeller is greater than that of the rear impeller.

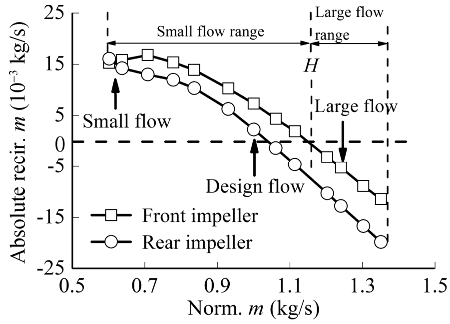

Fig. 10 Recirculation flow comparisons between front and rear impeller at design speed

The circumferential distribution of the recirculation flow

The recirculation flow of the both sides of the impeller is different at the stable operating conditions and design point. For the front impeller, the radial velocity of the bleed slot represents the recirculation flow, and the static pressure and the radial velocity at the middle position of the bleed slot are analyzed. The ten values are normalized by the circumferential average value respectively corresponding to the $V_r/\overline{V}_r$ and $P/\overline{P}$, Fig. 11 describes the results at three points, θ represents the circumferential angle referring to Fig. 4. The radial velocity and the static pressure are uneven along circumferential direction. The non-axisymmetric structure of the volute leads to the circumferential distribution of the static pressure [17, 19], Yang [20] detailed studied the static pressure distribution, and the circumferential distribution also changes at various operating conditions. At large flow, the circumferential distribution of the static pressure has the large non-uniform extent, which diminished with the decrease of the flow rate.

At the large flow condition, the circumferential distribution characteristics of the radial velocity at bleed slot was opposite to that of the static pressure from the Fig. 11(a). Due to the air flows into the impeller passage, the static pressure is took as the back pressure having a blocking effect. Therefore, the lower the static pressure, the higher the radial velocity. However, the air flows out to the inlet from the impeller at the design point, as shown in Fig. 11(b), and the static pressure of the bleed slot driven air flow through the duct. The higher static pressure area corresponds with the higher radial velocity. The small operating point has the similar variation trend

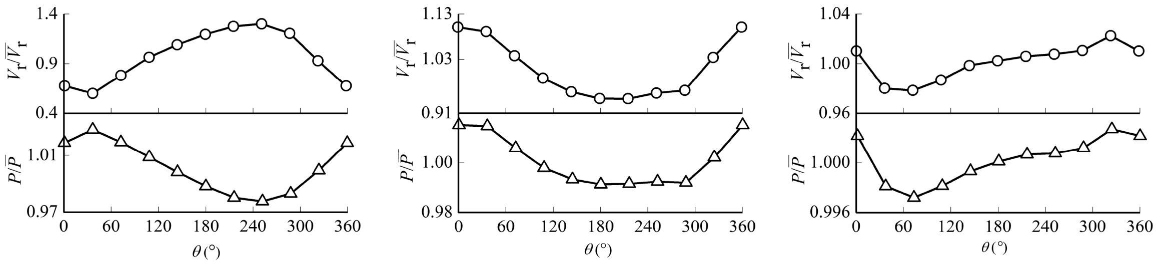

(a) Large flow (b) Design flow (c) Small flow

Fig. 11 Static pressure and radial velocity circumferential distribution lines at bleed slot of the front impeller in three operating conditions

with the design point at Fig. 11(c). The distribution of the radial velocity at three points describes that the static pressure distribution of the bleed slot determines the recirculation flow of the front impeller.

Table 1 compares the circumferential non-uniform extent of the radial velocity at three operating conditions, and the values at large flow rate are more than that of the other points, which has the less uniformity. The circumferential non-uniform extent of the static pressure gradually decreases with the lowing mass flow. Those phenomena illustrates that the circumferential non-uniform extent of the static pressure determines the recirculation velocity distribution with the flow decreases. The recirculation device reduces the circumferential non-uniform extent of the flow field at the large flow rate. The higher static pressure area at impeller outlet corresponds to the lower inlet mass flow, and the flow from the slot also decreased. Due to the flow is the sum of the inlet flow and slot flow, the slot aggravates the uneven distribution of the flow field at large flow condition.

Table 1 The non-uniform extent comparisons of front impeller in three operating conditions

Condition	$((V_r)_{max}-(V_r)_{min})/\bar{V}_r$	$(P_{max}-P_{min})/\bar{P}$
Large flow	0.59	0.051
Design flow	0.16	0.024
Small flow	0.04	0.006

Fig. 12 plots the static pressure and the radial velocity distribution of the rear impeller in three operating points. The variation law is similar with the front impeller. The correspondence between the static pressure and the radial velocity are similar at both side of impeller, but the variation lines around the slot position are different. The bent duct installed about 240°–300° at rear impeller results in the low static pressure area. The flow field distortion leads to the changed circumferential distribution of the static pressure at bleed slot. At three operating points, the normalized pressure and the velocity roughly have the same change trend but can't match very well, the recirculation flow of the bleed slot is also affected by the non-annular upstream slot and the inlet bent duct.

The circumferential non-uniform extent of the rear impeller, as shown in Table 2, are obviously more than that of the front impeller at three operating points, and the circumferential non-uniform extent of the radial velocity doesn't decrease with the lowering of the flow. Therefore, the uneven circumferential distribution of the radial velocity at rear impeller is determined by the inlet flow field distortion, the non-circular upstream slot and the non-axisymmetric structure of the volute.

The flow allocation at branch ducts of the rear impeller

Fig. 13 describes the flow allocation of the rear branch ducts with the total flow, the left flow is more than the

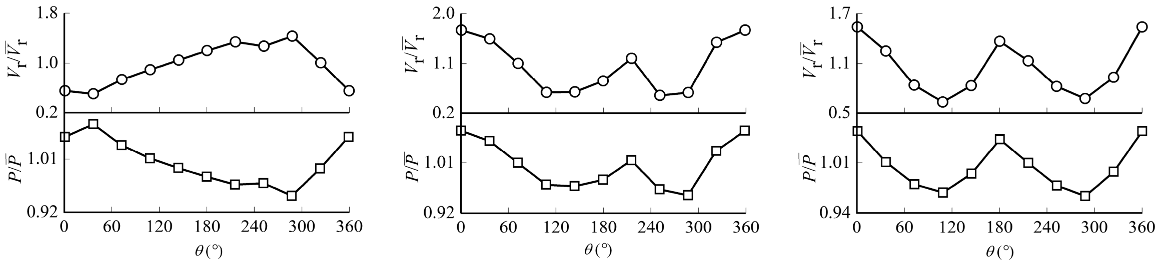

(a) Large flow (b) Design flow (c) Small flow

Fig. 12 Static pressure and radial velocity circumferential distribution lines at bleed slot of the rear impeller in three operating conditions

Table 2 The non-uniform extent comparisons of rear impeller in three operating conditions

Condition	$((V_r)_{max}-(V_r)_{min})/\overline{V}_r$	$(P_{max}-P_{min})/\overline{P}$
Large flow	0.93	0.122
Design flow	1.18	0.098
Small flow	0.91	0.091

right flow at large flow, and the small flow condition has a contrary tendency. The circumferential distribution of static pressure inside the compressor can interpret those phenomena. The non-symmetrical structure of the volute determines the uneven static pressure distribution, and every passage has different mass flow. The impeller passage, corresponding the higher static pressure of the diffuser and volute, has lower mass flow, and the circumferential uneven distribution changes at various operating points.

The uneven distribution inside the compressor not only influence the passage flow but also affect the branch duct flow of the rear impeller. The right branch has the lower flow because of the higher static pressure, but the small flow condition has an inverse pattern.

Fig. 14 describes the flow difference of both upstream slots of the rear impeller. The left upstream slot has the higher flow than that of the right slot at large flow, but the small flow has an inverse results. The increasing rate of the recirculation flow has a slowing trend as the flow decreases within the small flow.

The circumferential distribution of the recirculation velocity and recirculation flow rate of the rear impeller

The circumferential distribution of the recirculation flow in rear impeller is further analyzed because of the different recirculation flow in branch ducts at various points. The different recirculation flow of both side ducts in upstream slot represents the uneven circumferential allocation of the recirculation flow, which is plotted by the axial velocity V_z, and the Fig. 15 describes the axial velocity contour at three points. The static pressure distribution of the cross-section along the duct is also analyzed to elaborate the influence on recirculation velocity V_z, and the velocity V_z has the negative value when the air flows into the impeller at large flow rate. Fig. 15(a) validates the results and the upper trace area has the positive value. The upstream slot of both sides has the same axial velocity distribution, but the circumferential distribution is different.

Without the influence of wall boundary, the axial velocity of the lower area is more than the upper area because of the higher static pressure in the lower area.

The axial velocity distribution of both upstream slot and the same slot is different at design speed from Fig. 15(b). The upper area has the higher axial velocity than that of the lower area. The maximum at left slot was less than that of the right slot. Corresponding to the static pressure distribution, the upper area and the left slot has

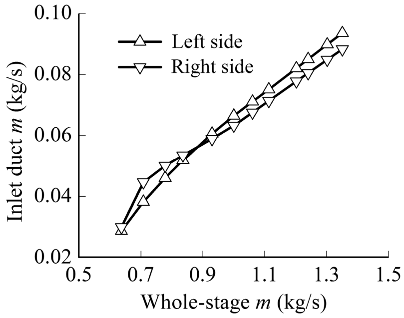

Fig. 13 Flow of left and right inlet duct of rear impeller

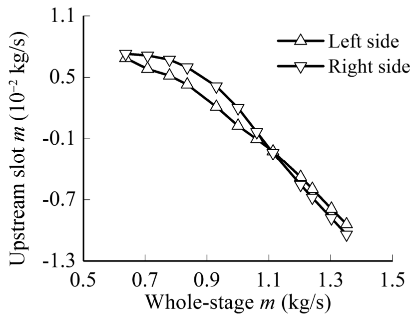

Fig. 14 Recirculation flow of left and right upstream slot of rear impeller

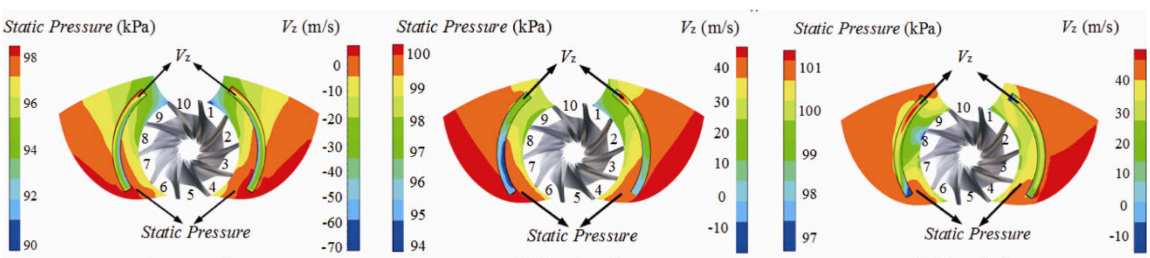

(a) Large flow (b) Design flow (c) Small flow

Fig. 15 Circumferential velocity contour at upstream slot of the rear impeller and static pressure contour at bent duct

the lower static pressure area. In the small flow condition, the upper area has the higher axial velocity in both slot from Fig. 15(c). The lower static pressure area lead to the higher axial velocity at the left slot. The circumferential distribution of the axial velocity in both upstream slot is different at three points from the above analysis, and the upper axial velocity is more than that in the lower area. The non-uniformity is influenced by the static pressure at inlet duct, and the shape of the inlet duct determined the static pressure around the slot. Therefor, the static pressure could be changed through adjusting the duct shape, and the axial velocity at upstream slot changes.

The difference of the axial velocity circumferential distribution that represents the upstream slot recirculation flow was determined from Fig. 15. The quantitative axial velocity circumferential distribution of the mean line in the upstream slot is plotted in Fig. 16, and the mean line is shown in Fig. 4. Because the air flows into the impeller passage, the axial velocity is negative. The axial velocity distribution has trace differences in both sides slot in Fig. 16(a), but the form is basically the same. The degradation rate of the axial velocity is different in the entire arc range and the axial velocity rapidly reduces at the upper area of the slot. The change process is determined by the static pressure distribution of the inlet ducts. According to the absolute V_z, the recirculation flow of the right side is more than that of the left side, Fig. 14 also confirm the results. The axial velocity distribution of both sides upstream at the mean line has the significant difference from the Fig. 16(b) at the design point. The right line has the positive value in the entire arc range, which indicate that the flow is pumped out from the impeller at the right slot, but the air flows into impeller in 0~50% arc range and is pumped out the inlet duct in 50%~100% arc range at the left slot, the right recirculation flow is more than the left slot. The upper axial velocity is more than that of the lower of the upstream slot at both sides from Fig. 16(c). The circumferential distribution of the axial velocity at upstream slot in rear impeller is determined by the static pressure distribution of the inlet duct from the above analysis.

The recirculation velocity is different at the upstream slot and bleed slot because of the changes of the recirculation velocity at the cavity.

Fig. 17 describes the radial velocity distribution at upstream slot of the front impeller, and the distribution has the same tendency with the static pressure distribution of the volute at three operating points, but there is a certain phase shift because of the circumferential position changes of the impellers during the back-propagation of the static pressure in the volute. The radial velocity distribution is more uniform at the upstream slot comparing with the rear impeller.

Fig. 18 shows the axial velocity distribution at different circumferential positions of the upstream slot within the rear impeller in three operating conditions, and Fig. 4 describes the detailed different circumferential positions. The axial velocity trend lines of both sides in the same circumferential positions remains broadly consistent at large flow condition from Fig. 18(a). The axial velocity decreases continuously from the inside (close to impeller) to outside (away from impeller), corresponding the maximum value and the minimum value, which is decided by the flow direction inside the duct. At large flow rate, the air flows into blade passages through the branch duct, and the air flows from the outside of the upstream slot to inside the inlet branch duct. Because of the inertia effect, the larger velocity is not generated in the outside of the upstream slot and the velocity gradually increases along the flow direction. So the velocity gradually increases from the outside of the upstream slot to the inside. However, the axial velocity distribution at both sides is different at the design flow rate from Fig. 18(b). The axial velocity of L3 is positive and the maximum locates at the middle slot, but the axial velocity of L1 and L2 are negative and has been increased after the first decrease at left

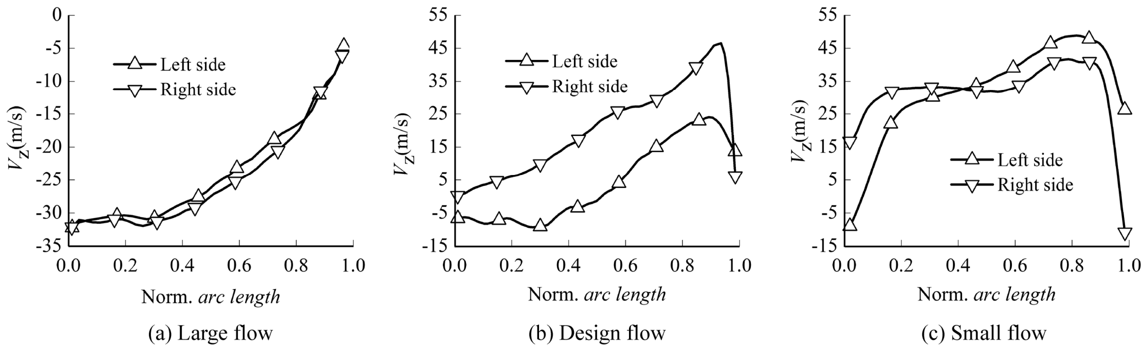

Fig. 16 Velocity distribution of upstream slot mean line of rear impeller in three operating conditions

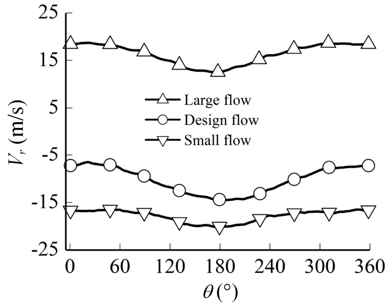

Fig. 17 Radial velocity distribution of upstream slot of front impeller

slot. The velocity distribution of three lines are roughly the same at right slot, they are symmetrical in the middle slot, which has the maximum velocity, the distribution is similar to the flow field between two parallel plates. With the increase of the recirculation flow, the velocity distribution of both sides are symmetrical at the middle slot in the small flow rate from Fig. 18(c). From the above analysis, the velocity distribution along the slot width tends to be symmetrical, namely the speed gradient is higher within the boundary layer and the axial velocity is the maximum in the middle slot.

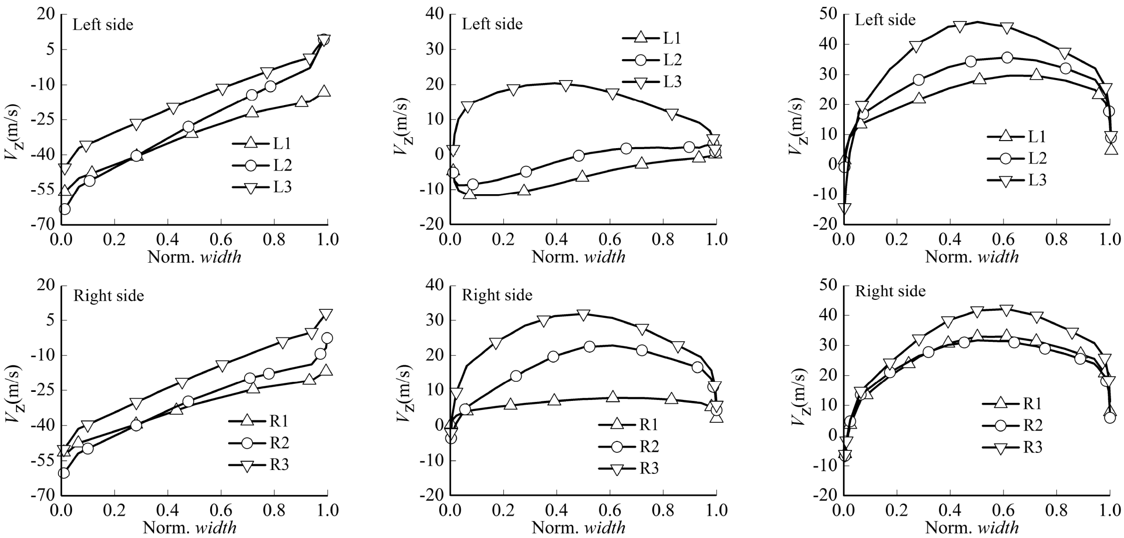

(a) Large flow (b) Design flow (c) Small flow

Fig. 18 Velocity distribution at different radii of upstream slot at both side impellers

Conclusions

This paper firstly analyzes the recirculation flow characteristics of double suction centrifugal compressor with non-axisymmetric recirculation device in stable operating conditions, and compared the difference of recirculation flow between both side impellers in the design speed. The circumferential non-uniform distribution of the recirculation velocity is presented and the causes of its formation is explained. Finally, the difference and the circumferential non-uniform distribution of the recirculation flow between branch ducts at the rear impeller are described. The main findings are summarized as follow:

The recirculation flow of the front impeller occupies 15.9 percent of front impeller flow. In the small flow range, with the decrease of the flow after the front impeller recirculation peak, the recirculation flow and the relative value of the four speeds all are on a downward trend, which indicates that the front impeller is far away from the stall boundary, but the recirculation flow of the rear impeller continuously increases. The recirculation flow of the rear impeller occupies 35.2 percent of rear impeller flow and is higher than the peak of the front relative recirculation flow. At the four speeds, the recirculation flow of the front impeller slightly increases with the decrease of the speed, while the recirculation flow of the rear impeller reduces. For the design speed, the recirculation flow of the rear impeller is more than that of the front impeller at the large flow rate. However, the recirculation flow of the front impeller is more than that of the rear impeller at the small flow rate.

The circumferential non-uniform distribution of the recirculation velocity always exist at three classical operating points for the front impeller. The non-uniform extent at the large flow rate is obviously more than the other points, and the small flow has the slight extent. The circumferential non-uniform extent of the static pressure determines the distribution of the recirculation velocity.

For the rear impeller, the circumferential non-uniform extent of the recirculation velocity is significantly greater than the front impeller at the same operating condition. The circumferential distribution of the recirculation ve-

locity changes at the cavity, but the circumferential non-uniform extent of the recirculation velocity does not reduce at the rear recirculation cavity with the decrease of the compressor flow rate. The three elements, including the flow distortion of the rear impeller, the circumferential non-symmetrical distribution of the upstream and the non-symmetrical structure of the volute, determine the circumferential non-uniform extent of the recirculation velocity of the rear impeller. And the circumferential distribution of the static pressure inside the impeller dominates the circumferential distribution of the recirculation velocity of the bleed slot.

In the design flow and the small flow, the recirculation velocity of the different circumferential positions of the mean line inside the upstream slot cross-section of the two branch ducts has significant difference, and the recirculation velocity also has major difference even though at the same recirculation slot. The static pressure distribution of the inlet duct determines the recirculation velocity distribution at the cross-section of the upstream slot.

Acknowledgements

This work was sponsored by the National Natural Science Foundation of China (No. 51276017) and the Specialized Research Fund for the Doctoral Program of Higher Education (No. 20131101110015), China.

References

[1] Arnold S. Single Sequential Turbocharger: A New Boosting Concept for Ultra-Low Emission Diesel Engines[J]. SAE International Journal of Engines, 2009(1): 232–239.

[2] DeRaad S, Fulton B, Gryglak A, et al. The New Ford 6.7L V-8 Turbocharged Diesel Engine[C]. SAE Paper, 2010, Michigan, USA, 2010-01-1101.

[3] Lei V M. Aerodynamics of a Centrifugal Compressor with a Double Side Impeller[C]. ASME Paper, 2011, Vancouver, Canada, GT2011-45215.

[4] Wangxia Wu, Ce Yang, Lei Jing, et al. Investigation of Impeller Operating Mode on Dual Boost Compressor. Journal of Engineering Thermophysics[J], 2015, 36(8): 1658–1661.

[5] Dickmann H P, Wimmel T S, Szwedowicz J, et al. Unsteady Flow in a Turbocharger Centrifugal Compressor: Three Dimensional Computational Fluid Dynamics Simulation and Numerical and Experimental Analysis of Impeller Blade Vibration[J]. Journal of Turbomachinery, 2006, 128(3): 455–465.

[6] Ce Yang, Shan Chen, Changmao Yang, et al. Inlet Recirculation Influence to the Flow Structure of Centrifugal Compressor[J]. Chinese Journal of Mechanical Engineering, 2010, 23(5): 647–654.

[7] Yang M, Martinez-Botas R, Zhang Y, et al. Investigation of Self-Recycling-Casing-Treatment (SRCT) Influence on Stability of High Pressure Ratio Centrifugal Compressor with a Volute[C]. ASME Paper, 2011, Vancouver, Canada, GT2011-45065.

[8] Peter Harley, Stephen Spence, Dietmar Filsinger, et al. Meanline Modeling of Inlet Recirculation in Automotive Turbocharger Centrifugal Compressors[J]. Journal of Tuobomachinery, 2015, 137(1): 011007-1-011007-9.

[9] Tamaki H. Effect of Recirculation Device on Performance of High Pressure Ratio Centrifugal Compressor[J]. Journal of Turbomachinery, 2010, 132(5): 1879–1889.

[10] Chen H, Lei V M. Casing Treatment and Inlet Swirl of Centrifugal Compressors[J]. Journal of Turbomachinery, 2013, 135(3): 928–931.

[11] Tamaki H. Effect of Recirculation Device with Counter Swirl Vane on Performance of High Pressure Ratio Centrifugal Compressor[C]. ASME Paper, 2011, Vancouver, Canada, GT2011-45360.

[12] Tamaki H, Unno M, Tanaka R, et al. Enhancement of Centrifugal Compressor Operating Range by Control of Inlet Recirculation with Inlet Fins[C]. ASME Paper, 2015, Montreal, Canada, GT2015-42154.

[13] Hunziker R, Dickmann H P, Emmrich R. Numerical And Experimental Investigation of a Centrifugal Compressor with an Inducer Casing Bleed System[J]. Proceedings of the Institution of Mechanical Engineers, Part A: Journal of Power and Energy, 2001, 215(6): 783–791.

[14] Hu Liangjun, Harold S, James Y, et al. Numerical and Experimental Investigation of a Compressor with Active Self-Recirculation Casing Treatment for a Wide Operation Range[J]. Proceedings of the Institution of Mechanical Engineers, Part D: Journal of Automobile Engineering, 2013, 227(9): 1227–1241.

[15] Gancedo M, Gutmark E, Guillou E. PIV Measurements of the Flow at the Inlet of a Turbocharger Centrifugal Compressor with Recirculation Casing Treatment near the Inducer[J]. Experiments in Fluids, 2016, 57(2): 1–19.

[16] Tamaki H, Xinqian Zheng, Yangjun Zhang. Experimental Investigation of High Pressure Ratio Centrifugal Compressor with Axisymmetric and Non-axisymmetric Recirculation Device[J]. Journal of Turbomachinery, 2013, 135(3): 420–431.

[17] Gu F, Engeda A. A Numerical Investigation on the Volute/Impeller Steady-state Interaction Due to Circumferential Distortion[C]. ASME Paper, 2001, New Orleans, USA, 2001-GT-0328.

[18] Yang M, Zheng X, Zhang Y, et al. Stability Improvement of High-Pressure-Ratio Turbocharger Centrifugal Compressor by Asymmetric Flow Control—Part I: Non-Axisymmetric Flow in Centrifugal Compressor[J]. Journal of Turbomachinery, 2013, 135(2): 210061–210069.

[19] Hagelstein D, Hillewaert K, Braembussche R A V D, et al. Experimental and Numerical Investigation of the Flow in a Centrifugal Compressor Volute[J]. Journal of Turbomachinery, 2000, 122(1): 22–30.

[20] Ce Yang, Yixiong Liu, Wangxia Wu, et al. Circumferential Flow Differences in the Double-Sided Centrifugal Compressor with Non-Balanced Inlets[C]. ASME Paper, 2016, Seoul, *South Korea*, GT2016-56167.

[21] Ce Yang, Lei Jing, Shan Chen, et al. Influence Study of Un-Equilibrium Inlet Condition to Flow Loss Characteristic of a Double-Sided Centrifugal Compressor[J]. Journal of Engineering Themophysics, 2016, 37(2), 264–267.

[22] Lei Jing, Ce Yang, Wangxia Wu, et al. Investigation of an Asymmetric Double Entry Centrifugal Compressor with Different Radial Impeller Matching for a Wide Operating Range[C]. ASME Paper, 2015, Montreal, Canada, GT2015-42892.